

Non-Hermitian symmetry breaking and Lee-Yang theory for quantum XYZ and clock models

Tian-Yi Gu^{1,2} and Gaoyong Sun^{1,2,*}

¹*College of Physics, Nanjing University of Aeronautics and Astronautics, Nanjing, 211106, China*

²*Key Laboratory of Aerospace Information Materials and Physics (NUAA), MIIT, Nanjing 211106, China*

Lee-Yang theory offers a unifying framework for understanding classical phase transitions and dynamical quantum phase transitions through the analysis of partition functions and Loschmidt echoes. Recently, this framework is extended to characterize quantum phase transitions of quantum Ising models by introducing the concepts of non-Hermitian parity-symmetry breaking and fidelity zeros. Here, we generalize the theory by studying a broad class of quantum models, including the XY, the XXZ, the XYZ, and the \mathbb{Z}_p clock models in one dimension, subject to a complex magnetic field. For the XY, XXZ and XYZ models, we find that the complex field breaks parity symmetry and induces oscillations of the ground state between the two parity sectors, giving rise to fidelity zeros within the ordered phases. For the \mathbb{Z}_3 clock model, the complex field splits the real part of the ground-state energy between the neutral sector ($q = 0$) and the charged sectors ($q = 1, 2$), while preserving the degeneracy within the charged sector. Fidelity zeros arise only after projecting out one of the charged sectors. In contrast, for the \mathbb{Z}_4 clock model, the ground state oscillates between the neutral sector ($q = 0$) and the charged sector ($q = 2$), which directly gives rise to fidelity zeros. Finite-size scaling of these zeros yields critical exponents in full agreement with analytical predictions, demonstrating that this approach is applicable not only to the Ising model with \mathbb{Z}_2 symmetry, but also to more general Heisenberg-type models and systems with higher discrete symmetries.

I. INTRODUCTION

Understanding phase transitions is one of the central topics in physics [1]. The logarithm of the partition function, which is equivalent to the Helmholtz free energy in the canonical ensemble, serves as the central thermodynamic potential, with its nonanalytic behavior marking the emergence of a phase transition [2, 3]. However, because the partition function is composed of statistical weights that are analytic functions, its logarithm cannot develop any nonanalyticity in a finite system [2]. To understand how phase transitions actually occur, Lee and Yang studied the partition function in finite systems under a complex magnetic field and developed a framework [4, 5] for characterizing phase transitions by analyzing its zeros, now known as Lee-Yang zeros [5]. For the ferromagnetic Ising model, Lee and Yang proved that all zeros lie precisely on the unit circle [2, 5, 6].

This compelling analysis of phase transitions and the distribution of zeros has attracted both theoretical [2, 7] and experimental [8, 9] interest over the past decades. The beauty of the Lee-Yang theory lies in identifying the zeros of the partition function in finite systems under a complex magnetic field, which appear only in systems with a real field in the thermodynamic limit. Fisher later extended this idea to study phase transitions by analyzing the zeros of the partition function (Fisher zeros) in the complex temperature plane [10]. Indeed, the key idea of analyzing the zeros of the partition function under a complex control parameter is quite general. For example,

beyond the Lee-Yang zeros and Fisher zeros, it has been shown that phase transitions can be explored through complex q in the q -state Potts model, giving rise to the concept of Potts zeros [11]. Moreover, for quantum systems subjected to a sudden quench, the Loschmidt echo, which is analogous to the partition function upon defining the imaginary time $\tau = it$ [12], is introduced to probe the system's dynamical behavior. The nonequilibrium phenomenon known as the dynamical quantum phase transition [12] arises in the time plane at the zeros of the Loschmidt echo.

The distribution of zeros is another research interest. Originally, the Lee-Yang unit circle theorem was discovered in the ferromagnetic Ising model [5]. It was subsequently extended to general Heisenberg spin models, showing that the theorem holds as long as the z - z coupling is ferromagnetic and dominant [13–16]. The distribution of zeros on the unit circle implies that they concentrate along the imaginary axis of the magnetic field. Furthermore, it is shown that at high temperatures $T > T_c$, a gap develops in the distribution, giving rise to branch points, referred to as the Yang-Lee edge singularity [17–21]. With decreasing temperature, the zeros approach and pinch the real axis [22], signaling a phase transition at $T = T_c$ in the thermodynamic limit. Recently, Lee-Yang zeros and the Yang-Lee edge singularity have been revisited both theoretically [23–34] and experimentally [35, 36].

In addition to classical and dynamical quantum phase transitions, quantum phase transitions [1, 37, 38] driven by quantum fluctuations are a central topic of broad interest in condensed matter physics. A natural extension of the Lee-Yang framework to quantum systems is to compute the partition function (or generating functions)

* Corresponding author: gysun@nuaa.edu.cn

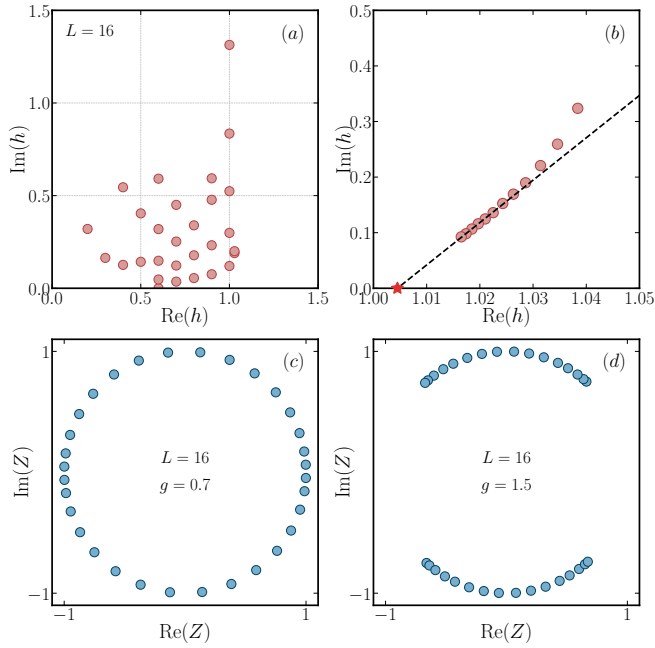


FIG. 1. Fidelity zeros and fidelity edges in the XY model at $\gamma = 0.8$. (a) Distribution of fidelity zeros in the complex- h plane for $L = 16$. Scatter points indicate the complex field values where the fidelity vanishes, with the critical point located at $\text{Re}(h) \approx 1$. (b) Finite-size scaling of the fidelity zeros as a function of system size L ranging from 10 to 32. Dark red dots represent the complex field h with the maximum real and minimum imaginary parts; the black dashed line shows the fitted curve, and the red star on the real axis marks the critical value $h = 1.005$. (c) and (d) Distributions of fidelity zeros in the complex field plane, expressed as $h = ge^{i\theta}$, with $L = 16$ for $g = 0.7$ and $g = 1.5$, respectively. All zeros lie on the unit circle $Z = e^{i\theta}$ with $\theta \in (0, 2\pi]$, and fidelity edges appear for $g = 1.5$.

of quantum many-body systems and analyze the distribution of zeros [39–51]. Nevertheless, it is well-known that the most direct approach to quantum phase transitions is through the ground state and its associated observables. A key question is whether the Lee-Yang framework can be captured from the ground states of quantum many-body systems. This question has been addressed in recent work [52] based on the concepts of non-Hermitian symmetry breaking and fidelity (overlap of two ground states) zeros. These zeros, examined in one- and two-dimensional ferromagnetic Ising models [52], confirm the validity of the Lee-Yang theory for quantum phase transitions via the ground states in the complex magnetic field plane. However, an important open question remains: does this fidelity-based Lee-Yang framework apply only to the ferromagnetic Ising model, or can it be extended to a broader class of quantum many-body systems, analogous to the generality of the original Lee-Yang theory for classical phase transitions?

In this work, we extend the framework developed in Ref. [52] to general quantum XYZ and \mathbb{Z}_p clock mod-

els. For the XYZ model, we show that the Lee-Yang theory holds by examining the XY, XXZ and XYZ models, where parity is broken by the complex field, as in the Ising model. In the \mathbb{Z}_p clock model, the \mathbb{Z}_p symmetry is similarly broken under the complex field. However, since the complex field cannot lift the degeneracy of ground states in the charged sectors ($q = 1, 2$), the fidelity-based Lee-Yang theory can only be formulated by projecting out one of these sectors in the $p = 3$ clock model. This work therefore generalizes the fidelity-based Lee-Yang theory to broader classes of models and higher discrete symmetries, demonstrating the wide applicability of the Lee-Yang framework.

II. XYZ MODEL

The general anisotropic Heisenberg Hamiltonian for the XYZ model with transverse and longitudinal magnetic fields is given by [14–16],

$$H = - \sum_{\langle i,j \rangle} (J_x S_i^x S_j^x + J_y S_i^y S_j^y + J_z S_i^z S_j^z) - \sum_i h_x S_i^x - \sum_i h_z S_i^z, \quad (1)$$

where J_x , J_y and J_z denote the real anisotropic couplings along the x , y and z directions, respectively, and h_x and h_z represent the complex transverse magnetic fields, defined as either $h_{x,z} = h_r + ih_i$ or $h_{x,z} = ge^{i\theta}$ in the x and z directions. Here, S_i^k ($k = x, y, z$) denotes the spin operators acting on site i , and the notation $\langle i,j \rangle$ specifies a summation over all nearest-neighbor pairs in the lattice. Throughout this work, periodic boundary conditions (PBCs) are imposed via $S_{L+1}^{x,y,z} = S_1^{x,y,z}$, with L denoting the total number of spins in the chain.

A. XY model

We first consider the ferromagnetic XY model under a complex transverse field applied along the z direction by setting $J_x, J_y > 0$, $J_z = 0$ and $h_x = 0$. The Hamiltonian of the anisotropic XY model is given by [53],

$$H = -J \sum_{\langle i,j \rangle} \left(\frac{1+\gamma}{2} \sigma_i^x \sigma_j^x + \frac{1-\gamma}{2} \sigma_i^y \sigma_j^y \right) - h \sum_i \sigma_i^z, \quad (2)$$

where, $J = (J_x + J_y)/4$, $\gamma = (J_x - J_y)/(J_x + J_y)$, $h = h_z/2$, and $\sigma_i^k = 2S_i^k$ ($k = x, y, z$) are Pauli matrices. When $\text{Im}(h) = 0$, the Hamiltonian describes the Hermitian quantum XY model. In this case, $J > 0$ indicates a ferromagnetic ordered phase, while $0 \leq \gamma \leq 1$ specifies the anisotropy strength. In the Hermitian regime, the XY model undergoes a quantum phase transition at $\text{Re}(h) = 1$. For $\gamma = 1$, it reduces to the Ising model. In contrast, when $\text{Im}(h) \neq 0$, the Hamiltonian becomes non-Hermitian.

The non-Hermitian XY model can be solved exactly by mapping spin operators onto spinless fermions [53]. To this end, it is convenient to rewrite Hamiltonian (2) using the spin ladder operators $\sigma_i^\pm = \frac{1}{2}(\sigma_i^x \pm i\sigma_i^y)$. The Hamiltonian (2) then becomes,

$$H = - \sum_{i=1}^L [\sigma_i^+ \sigma_{i+1}^- + \sigma_i^- \sigma_{i+1}^+ + \gamma(\sigma_i^+ \sigma_{i+1}^+ + \sigma_i^- \sigma_{i+1}^-)] - h \sum_{i=1}^L (2\sigma_i^+ \sigma_i^- - 1). \quad (3)$$

The Jordan-Wigner transformation, which maps spin-1/2 particles to spinless fermions, yields the following relations,

$$\begin{aligned} \sigma_i^+ &= c_i^\dagger \exp \left[i\pi \sum_{j=1}^{i-1} c_j^\dagger c_j \right] = c_i^\dagger \left(\prod_{j=1}^{i-1} \sigma_j^z \right), \\ \sigma_i^- &= \exp \left[-i\pi \sum_{j=1}^{i-1} c_j^\dagger c_j \right] c_i = \left(\prod_{j=1}^{i-1} \sigma_j^z \right) c_i, \\ \sigma_i^z &= 2c_i^\dagger c_i - 1, \end{aligned} \quad (4)$$

where c_i^\dagger and c_i are fermionic creation and annihilation operators satisfying the anticommutation relations $\{c_i^\dagger, c_j\} = \delta_{ij}$ and $\{c_i, c_j\} = 0$. It is important to note that this transformation maps the original periodic boundary conditions (PBCs) to either PBCs or antiperiodic boundary conditions, depending on whether the system contains an odd or even number of particles. In the following analysis, we consider an even number of particles, giving the Hamiltonian,

$$\begin{aligned} H_{\text{JW}} = & - \sum_{i=1}^L \left[(c_i^\dagger c_{i+1} + c_{i+1}^\dagger c_i) + \gamma (c_i^\dagger c_{i+1}^\dagger + c_{i+1} c_i) \right] \\ & + 2h \sum_{i=1}^L c_i^\dagger c_i. \end{aligned} \quad (5)$$

Applying the Fourier transformation,

$$c_j = \frac{1}{\sqrt{L}} \sum_k b_k e^{ikj}, \quad c_j^\dagger = \frac{1}{\sqrt{L}} \sum_k b_k^\dagger e^{-ikj}, \quad (6)$$

the Hamiltonian becomes,

$$H_{\text{FT}} = - \sum_k \left[2(\cos k - h)b_k^\dagger b_k + i\gamma \sin k (b_k^\dagger b_{-k}^\dagger + b_k b_{-k}) \right] \quad (7)$$

with k taking the values $k = 2n\pi/L$ for $n = -L/2 + 1, \dots, L/2$. By further applying the Bogoliubov transformation,

$$\begin{aligned} a_k &= \cos \theta_k b_k - i \sin \theta_k b_{-k}^\dagger, \\ a_{-k}^\dagger &= \cos^* \theta_k b_{-k}^\dagger - i \sin^* \theta_k b_k, \end{aligned} \quad (8)$$

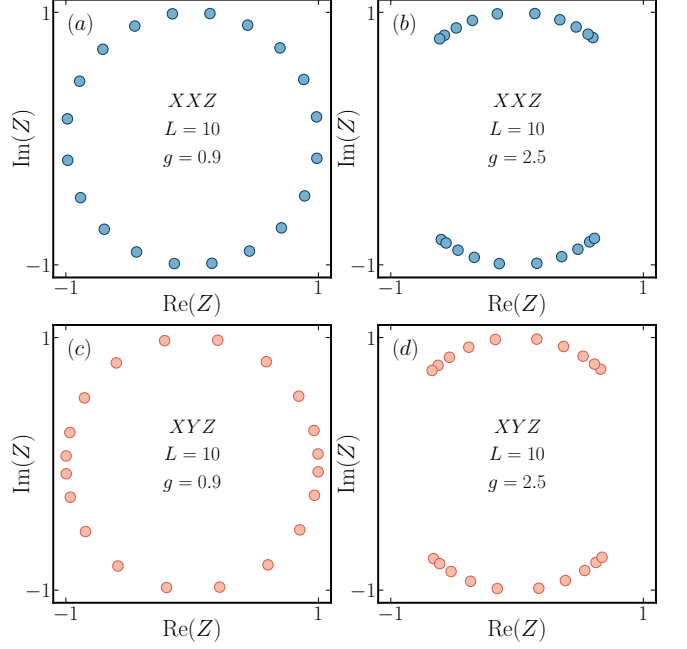


FIG. 2. Distributions of fidelity zeros in the complex field plane for the XXZ and XYZ models, with $h = ge^{i\theta}$. (a)-(b) Fidelity zeros for the XXZ model with $L = 10$ for $g = 0.9$ and $g = 2.5$, respectively. (c)-(d) Fidelity zeros for the XYZ model with the same parameters as in (a)-(b). All zeros lie on the unit circle $Z = e^{i\theta}$ with $\theta \in (0, 2\pi]$, and fidelity edges appear for $g = 2.5$.

with the Bogoliubov angle θ_k defined by $\cos 2\theta_k = (h - \cos \theta_k)/\sqrt{(\cos k - h)^2 + \gamma^2 \sin^2 k}$, the Hamiltonian (7) is diagonalized as,

$$H_{\text{BG}} = \sum_{k>0} 2\epsilon_k (a_k^\dagger a_k + a_{-k}^\dagger a_{-k} - 1). \quad (9)$$

where the operators a_k and a_k^\dagger are fermionic in momentum space and satisfy the same anticommutation relations as b_k and b_k^\dagger . The energy spectrum of the Hamiltonian is given by,

$$\epsilon_k = \sqrt{(\cos k - h)^2 + \gamma^2 \sin^2 k}, \quad (10)$$

with the ground state denoted as,

$$|\Psi_0(h)\rangle = \prod_{k>0} (\cos \theta_k + i \sin \theta_k c_k^\dagger c_{-k}^\dagger) |0\rangle. \quad (11)$$

The fidelity between h and h' is given by [52],

$$F(h, h') = \prod_{k>0} |(\cos^* \theta'_k \cos \theta_k + \sin^* \theta'_k \sin \theta_k)|. \quad (12)$$

It is worth noting that for an odd number of fermions, the ground-state energy and fidelity can be directly computed using the allowed k values $k = \pm(2n-1)\pi/L$, for $n = 1, \dots, L/2$.

We analytically calculate the ground-state fidelity of the XY model by varying the real part of the complex magnetic field h for $L = 16$ and $\gamma = 0.8$, and show the corresponding distribution of fidelity zeros in Fig. 1, with $J = 1$ fixed throughout the numerical simulations. As illustrated in Fig. 1(a), fidelity zeros appear in the system when $\text{Re}(h) < \text{Re}(h_L)$, while no zeros are observed for $\text{Re}(h) > \text{Re}(h_L)$. This behavior indicates that a quantum phase transition occurs at $\text{Re}(h_L)$. To study the finite-size scaling of fidelity zeros near the critical point, we first define h_L as the complex field h with the largest real part and the smallest imaginary part in our finite-size analysis. The finite-size scaling of both $\text{Re}(h_L)$ and $\text{Im}(h_L)$ is analyzed using the relation [52],

$$h_L = h_c + aL^{-1/\nu}, \quad (13)$$

where h_c and a are fitting parameters, and ν denotes the critical exponent of the correlation length. The scaling behavior of fidelity zeros in the XY model is shown in Fig. 1(b) for system sizes L ranging from 10 to 32. With increasing L , the critical points h_L converge such that the real part approaches the real axis and the imaginary part vanishes in the thermodynamic limit, resulting in the critical point $h_c = 1.005$ and $\nu = 1$.

We further examine the distribution of fidelity zeros in the complex magnetic field $h = ge^{i\theta}$ for $L = 16$ [c.f. Fig. 1(c) and (d)]. These zeros are computed for $g = 0.5$ and $g = 1.5$, while θ is varied over the interval $(0, 2\pi]$. By introducing the fugacity $Z = e^{i\theta}$, we observe that the zeros lie on the unit circle in the complex- h plane. For $g < h_c$, they are uniformly distributed along the circle; in contrast, for $g > h_c$, they condense into two circular arcs separated by a well-defined gap. These observations confirm that the Lee-Yang theory also holds for the XY model, as previously demonstrated for the transverse field Ising model [52].

In the case $J_x = J_y \neq J_z$ and $h_z = 0$, the system reduces to the XXZ model under a transverse field along the x direction. When $J_x = J_y < 0$ and $J_z/J_x < -1$, the system undergoes a phase transition from a ferromagnetic to a paramagnetic phase [54]. Furthermore, for the general XYZ model with $J_x \neq J_y \neq J_z$ and $h_z = 0$, a ferromagnetic-to-paramagnetic phase transition also occurs when the coupling $J_z > 0$ is dominant. Numerical simulations of the XXZ and XYZ models, presented in Fig. 2, further support the validity of the Lee-Yang framework in characterizing quantum phase transitions in general spin systems.

III. CLOCK MODEL

We have shown that the fidelity-based Lee-Yang framework is valid for the general spin-1/2 XYZ model. In the following, we extend this theory to the \mathbb{Z}_p clock model. The one-dimensional quantum \mathbb{Z}_p clock model

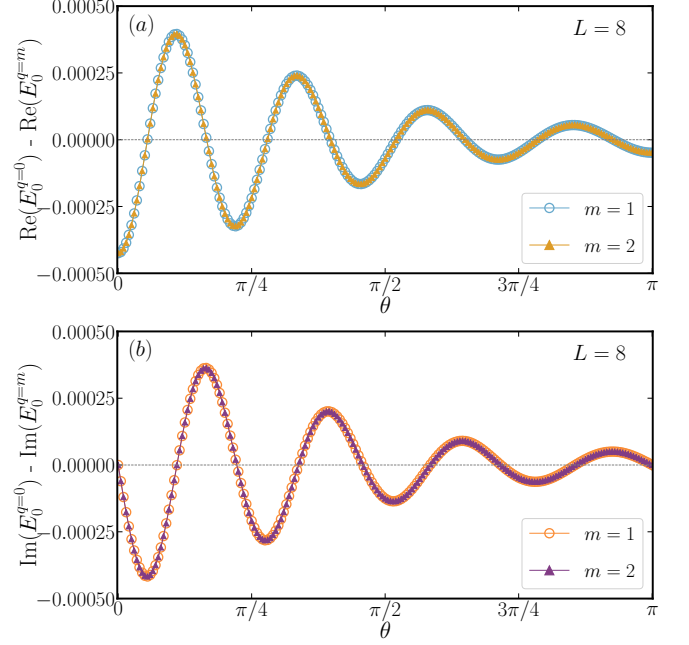


FIG. 3. Ground-state energy differences of the clock model in different symmetry sectors for $L = 8$ at $g = 0.5$. (a) Real part of the ground-state energy difference, $\text{Re}(E_0^{q=0}) - \text{Re}(E_0^{q=1,2})$ between the $q = 0$ and $q = 1, 2$ symmetry sectors as a function of θ . (b) Imaginary part of the ground-state energy difference, $\text{Im}(E_0^{q=0}) - \text{Im}(E_0^{q=1,2})$ between the $q = 0$ and $q = 1, 2$ symmetry sectors as a function of θ . The numerical results are obtained under a complex transverse field $h = ge^{i\theta}$ with $\theta \in [0, \pi]$.

is described by the Hamiltonian [55–60]:

$$H = -J \sum_{j=1}^L (V_{j+1}^\dagger V_j + V_j^\dagger V_{j+1}) - h \sum_{j=1}^L (U_j + U_j^\dagger), \quad (14)$$

where J denotes the coupling strength and h represents the complex transverse field. The quantum clock model exhibits a second-order phase transition for $p \leq 4$, whereas it undergoes a Berezinskii–Kosterlitz–Thouless transition for $p > 5$ [57]. In the following, we restrict our analysis to the second-order phase-transition regime. For $p = 2$, the quantum clock model is exactly equivalent to the transverse-field Ising chain. For $p = 3$, the operators V_j and U_j are defined by,

$$V_j = \begin{pmatrix} 0 & 1 & 0 \\ 0 & 0 & 1 \\ 1 & 0 & 0 \end{pmatrix}, U_j = \begin{pmatrix} 1 & 0 & 0 \\ 0 & \omega & 0 \\ 0 & 0 & \omega^2 \end{pmatrix}, \quad (15)$$

respectively, where $\omega = e^{2\pi i/3}$ and $(V_j)^3 = (U_j)^3 = \mathbb{1}$. Here, we impose $J = 1$ and periodic boundary conditions $V_{L+1} = V_1$. For a real field $\text{Im}(h) = 0$, the \mathbb{Z}_3 clock model undergoes a phase transition at the critical point $\text{Re}(h) = 1$, from a \mathbb{Z}_3 -symmetric gapped ordered phase to a gapped disordered phase, with the correlation-length critical exponent $\nu = 5/6$ [57].

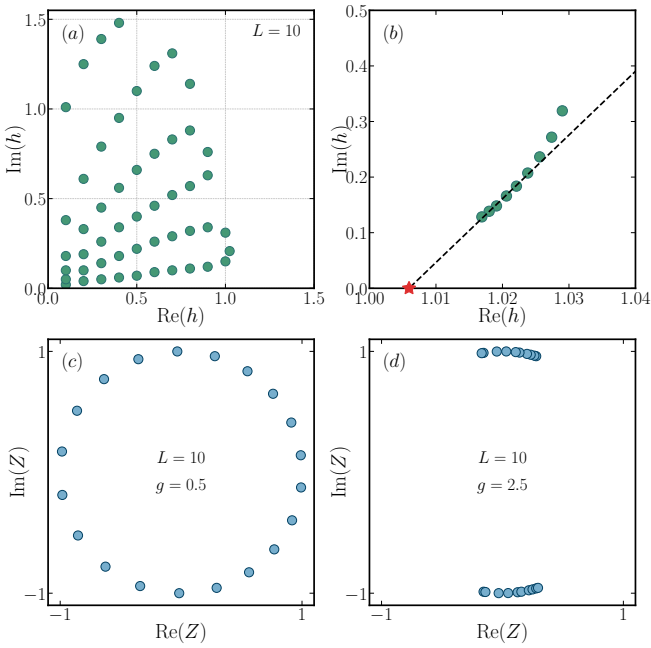


FIG. 4. Fidelity zeros and fidelity edges in the clock model. (a) Distribution of fidelity zeros in the complex- h plane for $L = 10$. The scatter points mark the complex field values at which the fidelity vanishes, with the critical point located at $\text{Re}(h) \approx 1$. (b) Finite-size scaling of the fidelity zeros as a function of system size L from 7 to 15. The green dots denote the complex field values with the largest real part and smallest imaginary part of the fidelity zeros; the black dashed line shows the fitted curve, and the red star on the real axis marks the critical value $h_c = 1.006$. (c)-(d) Fidelity-zero distributions in the complex-field plane for $L = 10$ for $g = 0.5$ and $g = 2.5$, respectively. All zeros lie on the unit circle $Z = e^{i\theta}$ with $\theta = (0, 2\pi]$; Fidelity edges appear for $g = 2.5$.

In the ordered phase, the three degenerate ground states lie in distinct symmetry sectors, determined by the many-body \mathbb{Z}_3 projector,

$$P_q = \frac{1}{3} \left[\mathbb{1} + \omega^{-q} \prod_j U_j + \omega^{-2q} \left(\prod_j U_j \right)^2 \right], \quad (16)$$

for the Hamiltonian labeled by $q = 0, 1, 2$. Specifically, $q = 0$ identifies the neutral sector, whereas $q = 1$ and $q = 2$ belong to the charged sectors.

However, when the external field is complex, for example $h = ge^{i\theta}$, it leads to the non-Hermitian symmetry-breaking and lifts the ground-state degeneracy, defined by the lowest real part of the complex energies. Notably, the complex field only lifts the degeneracy between the neutral sector ($q = 0$) and the charged sectors ($q = 1, 2$), while the two ground-state energies within the charged sectors ($q = 1, 2$) remain degenerate, as shown in Fig. 3. Because of this degeneracy, the ground state cannot be uniquely assigned to either the $q = 1$ or $q = 2$ sector. Consequently, fidelity is ill-defined, as the ground

state forms a superposition of states from the $q = 1$ or $q = 2$ sectors. To lift this degeneracy and select a unique charged sector, we introduce an additional projector $P' = \mathbb{1} - P_2$, which completely projects out the $q = 2$ sector. This results in a clear non-Hermitian symmetry-breaking between the $q = 0$ and $q = 1$ sector, which can be detected through fidelity zeros.

To validate our results, we numerically compute the fidelity zeros for a system of size $L = 10$ in the complex field plane. The zeros are found exclusively within the ordered phase and vanish abruptly in the disordered phase, as shown in Fig. 4(a). For $L = 10$, the phase transition is located at $\text{Re}(h_L) = 1.0238$. As the lattice size increases, the real part of h approaches the real axis while the imaginary part vanishes in the thermodynamic limit, yielding a critical point $h_c = 1.006$ with $\nu = 5/6$, as illustrated in Fig. 4(b) through the finite-size scaling according to Eq. (13). Furthermore, under the condition $h = gZ = e^{i\theta}$, all fidelity zeros lie on the unit circle in the complex- Z plane, with a total of $2L$ zeros. Their distribution, however, differs significantly between the ordered and disordered phases. For $g < h_c$, the zeros are distributed almost uniformly along the circle [c.f. Fig. 4(c)], whereas for $g > h_c$, they coalesce into two distinct arcs [c.f. Fig. 4(d)]. These results demonstrate that fidelity-based Lee-Yang approach is applicable to models with higher \mathbb{Z}_3 symmetries.

For $p = 4$ quantum clock model, the operators V_j and U_j are given by

$$V_j = \begin{pmatrix} 0 & 1 & 0 & 0 \\ 0 & 0 & 1 & 0 \\ 0 & 0 & 0 & 1 \\ 1 & 0 & 0 & 0 \end{pmatrix}, \quad U_j = \begin{pmatrix} 1 & 0 & 0 & 0 \\ 0 & \omega & 0 & 0 \\ 0 & 0 & \omega^2 & 0 \\ 0 & 0 & 0 & \omega^3 \end{pmatrix}, \quad (17)$$

respectively, where $\omega = e^{2\pi i/4} = i$ and $(V_j)^4 = (U_j)^4 = \mathbb{1}$. For the \mathbb{Z}_4 clock model, the many-body projector can be constructed in close analogy to the \mathbb{Z}_3 case, and is explicitly expressed as

$$P_q = \frac{1}{4} [\mathbb{1} + \mathbb{T} + \mathbb{T}^2 + \mathbb{T}^3]. \quad (18)$$

Here, $\mathbb{T} = \omega^{-q} \prod_j U_j$, $q = 0$ is the neutral sector, and $q = 1, 2, 3$ are the charged sectors.

For the \mathbb{Z}_4 clock model, the phase transition occurs at $\text{Re}(h) = 1$ with critical exponent $\nu = 1$ under a real field [57]. In the presence of a complex field, non-Hermitian symmetry breaking lifts the ground-state degeneracy. Specifically, the complex field splits the spectrum among the neutral sector ($q = 0$), the charged sector ($q = 2$), and the pair of degenerate charged sectors ($q = 1, 3$). As a consequence, the ground state is effectively governed by the competition between the $q = 0$ and $q = 2$ sectors, giving rise to fidelity zeros that provide a clear signature of the phase transition.

We numerically calculate the fidelity zeros in the complex-field plane for a system of size $L = 8$, as shown in Fig. 5(a). The zeros are prominently distributed around

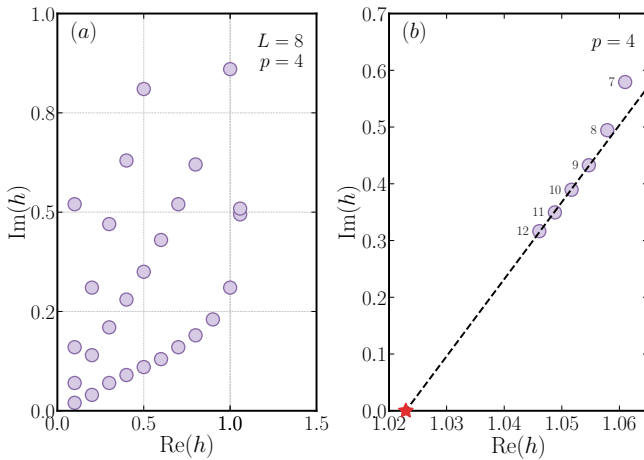


FIG. 5. Fidelity zeros in the \mathbb{Z}_4 clock model. (a) Distribution of fidelity zeros in the complex- h plane for $L = 8$. The scatter points mark the complex field values at which the fidelity vanishes, with the critical point located around $\text{Re}(h) \approx 1$. (b) Finite-size scaling of the fidelity zeros as a function of system size L from 7 to 12. The purple dots denote the complex field values with the largest real part of the fidelity zeros; the black dashed line shows the fitted curve, and the red star on the real axis marks the critical value $h_c = 1.023$.

$\text{Re}(h) = 1$. For $L = 8$, the finite-size transition point is found at $\text{Re}(h_L) = 1.0579$. Remarkably, fidelity zeros occur only in the region $\text{Re}(h) < \text{Re}(h_L)$, whereas they are absent for $\text{Re}(h) > \text{Re}(h_L)$. Applying the finite-size scaling analysis of Eq. (13), we determine the critical point $h_c = 1.023$ with the correlation-length critical exponent $\nu = 1$, as illustrated in Fig. 5(b). These findings provide further evidence that the fidelity-zero framework can be

systematically extended to models with higher discrete symmetries.

IV. CONCLUSION

In summary, we have generalized the Lee-Yang theory based on fidelity zeros to both the XYZ model and the \mathbb{Z}_3 clock model. The fidelity zeros in these systems, arising from non-Hermitian symmetry breaking, exhibit distinct distributions in the ordered and disordered phases, consistently obey the Lee-Yang theorem, and faithfully signal the phase transition. Our results show that this approach is not only effective for the anisotropic XYZ model but also capable of capturing criticality in systems with higher discrete symmetries, such as the \mathbb{Z}_p clock model. Consequently, the fidelity-based Lee-Yang framework provides a simpler implementation with robust numerical accuracy for identifying quantum phase transitions, thereby opening avenues for applying the Lee-Yang formalism to a broader class of correlated quantum systems. A promising direction for future work is to explore its extension to continuous symmetry-breaking cases, such as $U(1)$ and $SU(2)$ symmetries.

V. ACKNOWLEDGMENTS

G.S. is appreciative of support from the NSFC under the Grants No. 11704186 and "the Fundamental Research Funds for the Central Universities, NO. NS2023055". T.-Y. G acknowledges support from the Postgraduate Research & Practice Innovation Program of NUAA under Grant No. xcjh20252113. This work is partially supported by the High Performance Computing Platform of Nanjing University of Aeronautics and Astronautics.

[1] S. Sachdev, *Quantum phase transitions* (Cambridge University Press, 1999).

[2] I. Bena, M. Droz, and A. Lipowski, Statistical mechanics of equilibrium and nonequilibrium phase transitions: the yang–lee formalism, *International Journal of Modern Physics B* **19**, 4269 (2005).

[3] Z. Wang, Y.-M. Ding, Z. Liu, and Z. Yan, Extracting the singularity of the logarithmic partition function, [arXiv:2506.16111](https://arxiv.org/abs/2506.16111) (2025).

[4] C.-N. Yang and T.-D. Lee, Statistical theory of equations of state and phase transitions. i. theory of condensation, *Physical Review* **87**, 404 (1952).

[5] T.-D. Lee and C.-N. Yang, Statistical theory of equations of state and phase transitions. ii. lattice gas and ising model, *Physical Review* **87**, 410 (1952).

[6] B.-B. Wei and R.-B. Liu, Lee-yang zeros and critical times in decoherence of a probe spin coupled to a bath, *Physical Review Letters* **109**, 185701 (2012).

[7] M. Heyl, Dynamical quantum phase transitions: a review, *Reports on Progress in Physics* **81**, 054001 (2018).

[8] X. Peng, H. Zhou, B.-B. Wei, J. Cui, J. Du, and R.-B. Liu, Experimental observation of lee-yang zeros, *Physical Review Letters* **114**, 010601 (2015).

[9] K. Brandner, V. F. Maisi, J. P. Pekola, J. P. Garrahan, and C. Flindt, Experimental determination of dynamical lee-yang zeros, *Physical Review Letters* **118**, 180601 (2017).

[10] M. E. Fisher, *The nature of critical points, in Lectures in Theoretical Physics* (vol VIIC, edited by W. E. Brittin, University of Colorado Press, 1965).

[11] S.-Y. Kim and R. J. Creswick, Density of states, potts zeros, and fisher zeros of the q-state potts model for continuous q, *Physical Review E* **63**, 066107 (2001).

[12] M. Heyl, A. Polkovnikov, and S. Kehrein, Dynamical quantum phase transitions in the transverse-field ising model, *Physical Review Letters* **110**, 135704 (2013).

[13] M. Suzuki, On the distribution of zeros for the heisenberg model, *Progress of Theoretical Physics* **41**, 1438 (1969).

[14] T. Asano, Lee-yang theorem and the griffiths inequality for the anisotropic heisenberg ferromagnet, *Physical Review Letters* **24**, 1409 (1970).

[15] T. Asano, Theorems on the partition functions of the heisenberg ferromagnets, *Journal of the Physical Society of Japan* **29**, 350 (1970).

[16] M. Suzuki and M. E. Fisher, Zeros of the partition function for the heisenberg, ferroelectric, and general ising models, *Journal of Mathematical Physics* **12**, 235 (1971).

[17] M. E. Fisher, Yang-lee edge singularity and ϕ 3 field theory, *Physical Review Letters* **40**, 1610 (1978).

[18] D. A. Kurtze and M. E. Fisher, Yang-lee edge singularities at high temperatures, *Physical Review B* **20**, 2785 (1979).

[19] J. L. Cardy, Conformal invariance and the yang-lee edge singularity in two dimensions, *Physical Review Letters* **54**, 1354 (1985).

[20] J. L. Cardy and G. Mussardo, S-matrix of the yang-lee edge singularity in two dimensions, *Physics Letters B* **225**, 275 (1989).

[21] B.-B. Wei, Probing yang-lee edge singularity by central spin decoherence, *New Journal of Physics* **19**, 083009 (2017).

[22] N. Ananikian and R. Kenna, Imaginary magnetic fields in the real world, *Physics* **8**, 2 (2015).

[23] S. Yin, G.-Y. Huang, C.-Y. Lo, and P. Chen, Kibble-zurek scaling in the yang-lee edge singularity, *Physical Review Letters* **118**, 065701 (2017).

[24] Q.-J. Ye, L. Zhuang, and X.-Z. Li, Dynamic nature of high-pressure ice vii, *Physical Review Letters* **126**, 185501 (2021).

[25] S.-K. Jian, Z.-C. Yang, Z. Bi, and X. Chen, Yang-lee edge singularity triggered entanglement transition, *Physical Review B* **104**, L161107 (2021).

[26] T. Sanno, M. G. Yamada, T. Mizushima, and S. Fujimoto, Engineering yang-lee anyons via majorana bound states, *Physical Review B* **106**, 174517 (2022).

[27] R. Shen, T. Chen, M. M. Aliyu, F. Qin, Y. Zhong, H. Loh, and C. H. Lee, Proposal for observing yang-lee criticality in rydberg atomic arrays, *Physical Review Letters* **131**, 080403 (2023).

[28] Q.-J. Ye and X.-Z. Li, Dynamic phase transition theory, *Science China Physics, Mechanics & Astronomy* **66**, 227212 (2023).

[29] X.-Y. Ouyang, Q.-J. Ye, and X.-Z. Li, Complex phase diagram and supercritical matter, *Physical Review E* **109**, 024118 (2024).

[30] M.-C. Lu, S.-H. Shi, and G. Sun, Dynamical signatures of the yang-lee edge singularity in non-hermitian systems, *Physical Review B* **111**, 054309 (2025).

[31] M. Xu, W. Yi, and D.-H. Cai, Characterizing the yang-lee zeros of the classical ising model through dynamic quantum phase transitions, *Physical Review A* **111**, 042204 (2025).

[32] W.-Y. Zhang, M.-Y. Mao, Q.-M. Hu, X. Zhao, G. Sun, and W.-L. You, Yang-lee edge singularity and quantum criticality in non-hermitian ppx model, *Physical Review B* **112**, 155135 (2025).

[33] Y.-M. Sun, W.-J. Yu, X.-Y. Wang, and L.-J. Zhai, Hybrid scaling mechanism of critical behavior in the overlapping critical regions of classical and quantum yang-lee edge singularities, *arXiv:2506.00919* (2025).

[34] Z.-M. Xu and R. B. Mann, Thermodynamic supercriticality and complex phase diagram for the ads black hole, *Physical Review Letters* **136**, 041402 (2026).

[35] H. Gao, K. Wang, L. Xiao, M. Nakagawa, N. Matsumoto, D. Qu, H. Lin, M. Ueda, and P. Xue, Experimental observation of the yang-lee quantum criticality in open quantum systems, *Physical Review Letters* **132**, 176601 (2024).

[36] Z. Lan, W. Liu, Y. Wu, X. Ye, Z. Yang, C.-K. Duan, Y. Wang, and X. Rong, Experimental investigation of lee-yang criticality using non-hermitian quantum system, *Chinese Physics Letters* **41**, 050301 (2024).

[37] S. L. Sondhi, S. Girvin, J. Carini, and D. Shahar, Continuous quantum phase transitions, *Reviews of Modern Physics* **69**, 315 (1997).

[38] M. Vojta, Quantum phase transitions, *Reports on Progress in Physics* **66**, 2069 (2003).

[39] P. Tong and X. Liu, Lee-yang zeros of periodic and quasiperiodic anisotropic xy chains in a transverse field, *Physical Review Letters* **97**, 017201 (2006).

[40] T. Kist, J. L. Lado, and C. Flindt, Lee-yang theory of criticality in interacting quantum many-body systems, *Physical Review Research* **3**, 033206 (2021).

[41] P. M. Vecsei, J. L. Lado, and C. Flindt, Lee-yang theory of the two-dimensional quantum ising model, *Physical Review B* **106**, 054402 (2022).

[42] P. M. Vecsei, C. Flindt, and J. L. Lado, Lee-yang theory of quantum phase transitions with neural network quantum states, *Physical Review Research* **5**, 033116 (2023).

[43] J. Liu, S. Yin, and L. Chen, Imaginary-temperature zeros for quantum phase transitions, *Physical Review B* **110**, 134313 (2024).

[44] Y. Liu, S. Lv, Y. Meng, Z. Tan, E. Zhao, and H. Zou, Exact fisher zeros and thermofield dynamics across a quantum critical point, *Physical Review Research* **6**, 043139 (2024).

[45] P. M. Vecsei, J. L. Lado, and C. Flindt, Lee-yang formalism for phase transitions of interacting fermions using tensor networks, *Physical Review B* **111**, 075134 (2025).

[46] H. Li, X.-H. Yu, M. Nakagawa, and M. Ueda, Yang-lee zeros, semicircle theorem, and nonunitary criticality in bardeen-cooper-schrieffer superconductivity, *Physical Review Letters* **131**, 216001 (2023).

[47] H. Li, Yang-lee zeros in quantum phase transitions: An entanglement perspective, *Physical Review B* **111**, 045139 (2025).

[48] Y. Meng, S. Lv, Y. Liu, Z. Tan, E. Zhao, and H. Zou, Detecting many-body scars from fisher zeros, *Physical Review Letters* **135**, 070402 (2025).

[49] J. Wang, E. Lv, X. Li, Y. Jin, and W. Li, Quantum supercritical crossover with dynamical singularity, *arXiv:2407.05455* (2024).

[50] R.-C. He, J.-X. Zeng, S. Yang, C. Wang, Q.-J. Ye, and X.-Z. Li, Revisiting the fermion sign problem from the structure of lee-yang zeros. i. the form of partition function for indistinguishable particles and its zeros at 0k, *arXiv:2507.22779* (2025).

[51] S. Lv, Y. Liu, E. Zhao, H. Zou, and T. Xiang, Giant bubbles of fisher zeros in the quantum xy chain, *arXiv:2602.05899* (2026).

[52] T.-Y. Gu and G. Sun, Fidelity zeros and lee-yang theory of quantum phase transitions, *Physical Review B* **113**, 014417 (2026).

[53] J. Pi and R. Lü, Phase diagram and quantum criticality of a non-hermitian xy model with a complex transverse field, *Journal of Physics: Condensed Matter* **33**, 345601 (2021).

[54] D. Dmitriev, V. Y. Krivnov, and A. Ovchinnikov, Gap generation in the xxz model in a transverse magnetic

field, *Physical Review B* **65**, 172409 (2002).

[55] G. Ortiz, E. Cobanera, and Z. Nussinov, Dualities and the phase diagram of the p-clock model, *Nuclear Physics B* **854**, 780 (2012).

[56] J. Chen, H.-J. Liao, H.-D. Xie, X.-J. Han, R.-Z. Huang, S. Cheng, Z.-C. Wei, Z.-Y. Xie, and T. Xiang, Phase transition of the q-state clock model: Duality and tensor renormalization, *Chinese Physics Letters* **34**, 050503 (2017).

[57] G. Sun, T. Vekua, E. Cobanera, and G. Ortiz, Phase transitions in the z_p and $u(1)$ clock models, *Physical Review B* **100**, 094428 (2019).

[58] J.-C. Tang, W.-L. You, M.-J. Hwang, and G. Sun, Dynamical scaling laws in the quantum q-state clock chain, *Physical Review B* **107**, 134303 (2023).

[59] X.-J. Yu, Dynamical phase transition and scaling in the chiral clock potts chain, *Physical Review A* **108**, 062215 (2023).

[60] L.-F. Yu, W.-L. Li, X.-J. Yu, and Z. Li, Emergent dynamical quantum phase transition in a z_3 symmetric chiral clock model, [arXiv:2411.03953](https://arxiv.org/abs/2411.03953) (2024).